

Lumped Disturbance Compensation using Extended Kalman Filter for Permanent Magnet Linear Motor System

Jonghwa Kim, Kwanghyun Cho, and Seibum Choi*

Abstract: In this paper, an extended Kalman filter is designed and applied to a feed-forward based lumped disturbance compensator which consists of position dependent functions for a permanent magnet linear synchronous motor system. In our previous research, a lumped disturbance model including the force ripple and the Coulomb friction force was developed and utilized as a feed-forward controller. To improve the performance of that model, following two studies are conducted. First, an initial position estimator is designed to create synchronization between the model and real disturbance. This step is necessary because almost all linear motor systems are equipped with an incremental encoder for position measurement. Second, to cancel out a slight variation in real disturbance, an adaptive controller in the form of coefficients adaptation is designed. These two studies are combined by a sixth order extended Kalman filter. To make a comparison, a recursive least squares filter and disturbance observer and its modified version are prepared. The effectiveness of the proposed scheme is verified by the overall disturbance shape, RMS position error and FFT analysis on the position error.

Keywords: Detent force, disturbance observer, extended Kalman filter, feed-forward compensation, force ripple, initial position, lumped disturbance, permanent magnet linear motor.

1. INTRODUCTION

Many industrial areas such as LED panel transportation and semi-conductor manufacturing, require high precision linear motion controlled systems. With a conventional rotary type motor as an actuator, transmission mechanisms are positively necessary to convert rotary motion to translational motion. This indirect structure inevitably produces some problems: backlash, hysteresis, poor energy efficiency and limited system bandwidth. To resolve these issues, direct-driven linear motor systems have been developed and used. However, paradoxically, in the absence of any indirect apparatus, the linear motor system becomes quite sensitive to model uncertainties and external disturbances.

Two representative disturbances in the motor driven system are the force ripple and the friction force. The friction force can be considered as a constant except for the very low speed region where the Stribeck effect [1] is notable. On the other hand, the force ripple can be categorized as the detent force and the reluctance force. The detent force originates from the mechanical structure. In permanent magnet motor systems, iron is sometimes in-

serted into the coils to obtain high thrust force and high power density. This means there is a mutual attraction between the stator and the rotor all the time regardless of operating conditions, even when the power is off. Therefore, this detent force is position dependent and also periodical. The reluctance force is also related to the structure of the motor system. The self-inductance of the coil in the mover is affected by the relative position of it with respect to the permanent magnets.

In the real system, there are some other additional factors that form the force ripple [2–4]. These factors are due to imperfections, such as uneven magnetic force among the permanent magnets and imperfect current waveform. Due to these factors, the force ripple has higher order harmonics (e.g., the 2nd, 4th, 6th and even the 12th order). Consequently, to achieve more precise motion control, analysis of the target plant system for its dominant harmonic order and corresponding magnitude should be conducted.

For more than a decade, there have been many studies to compensate for this force ripple. However, some researches [5–8] have used only the fundamental harmonic term without any additional analysis to determine whether

Manuscript received October 9, 2014; revised June 19, 2015; accepted October 7, 2015. Recommended by Associate Editor Xiaojie Su under the direction of Editor Yoshito Ohta. This research was supported by the MSIP (Ministry of Science, ICT&Future Planning), Korea, under the CITRC (Convergence Information Technology Research Center) support program (NIPA-2014-H0401-14-1001) supervised by the NIPA (National IT Industry Promotion Agency) and the National Research Foundation of Korea (NRF) grant funded by the Korea government (MSIP) (No.2010-0028680).

Jonghwa Kim, Kwanghyun Cho, and Seibum Choi are with the School of Mechanical Engineering, KAIST, 291 Daehak-ro (373-1 Guseong-dong), Yuseong-gu, Daejeon 305-701 Korea (e-mails: {jjong52, khcho08, sbchoi}@kaist.ac.kr).

* Corresponding author.

the higher order harmonics are negligible or not. Meanwhile, some researchers concluded that up to the 6th order harmonics should be compensated for precise motion control [3]. Further, Bascetta *et al.* tried to compensate for the force ripple with the information of up to the 10th order harmonics [4]. In our previous research [2], more than 87% of the force ripple was supposed to be eliminated by accurate compensation for up to the 4th order harmonics.

Besides, due to the imperfections of a linear motor system, the force ripple is not exactly periodic, but ‘periodic-like’ (i.e., the magnitude, offset and period of the force ripple are slightly different along the position). This means that the coefficient of each harmonic order for the force ripple compensation should be different along the motor position. However, this effect has not been handled sufficiently, and some experiments have been conducted within the range of a single pole pitch of permanent magnet [5, 9, 10] or just 2 or 3 poles [6, 7, 11–13]. One study sought to find each single coefficient for each harmonics compensation regardless of translator position for the whole operating range of 0.25m [14]. In that case, the performance of motion control would naturally get deteriorated along with the non-periodicity of the imperfection. Another study adopted a recursive least squares method for an adaptive control approach [6]. The performance was not quite satisfactory since the compensating coefficients of the force ripple can not change fast enough from a permanent magnet to the next one.

In general, the required position error boundary in a linear motor system is very tight (e.g., a few micrometers) for using an absolute encoder, and therefore the incremental encoder is utilized as a position sensor. This means, from the feed-forward compensation point of view, information on the absolute starting (initial) position is necessary and should be reflected. In this study, we did this with an extended Kalman filter.

Some studies [4, 15] suggested a look-up table strategy through experimental data fitting, which might be simpler and easier than analyzing and calculating the position dependent sinusoidal function. It might also be convenient to consider very high harmonics order (e.g., up to the 10th order harmonics in [4]). However, the look-up table method has difficulties while adjusting the table values by any adaptive control scheme. In addition, the information about the starting position is necessary for this method too.

The disturbance observer is utilized in some studies [10–12, 16], but as analyzed in our previous study [2], there are some critical weak points. In general, a Q-filter (a kind of low-pass-filter) is attached to the end of a disturbance observer to attenuate the effect of measurement noise. The cutoff frequency of the Q-filter is determined by considering the system bandwidth and sensor properties, which is usually constant irrespective of the operating conditions such as traveling speed and moving range.

Meanwhile, the force ripple frequency is increased proportional to the motor speed because of the position dependency. At a high speed, some force ripple harmonics may exceed the Q-filter bandwidth and they will not be compensated through the disturbance observer. Even when the Q-filter bandwidth is not exceeded, there are always some amount of phase lag due to the filtering effect.

To overcome all these limitations, we propose a new feed-forward based lumped disturbance compensating method. On the basis of the disturbance model we previously devised in [2], an extended Kalman filter is designed and applied to reflect the starting position and to adjust the coefficient magnitude of the sinusoidal disturbance model. As a nonlinear filter similar to the extended Kalman filter, an unscented Kalman filter or a particle filter in stochastic approach might be another candidate [17–20]. In this case, since we already have the ripple model, the extended Kalman filter utilizing the model is adopted.

The rest of this paper is organized as follows. The base disturbance model is introduced and summarized in Section 2. The extended Kalman filter is designed in Section 3. The recursive least squares algorithm and the delta disturbance observer are described in Section 4. Then simulation results and experimental results are shown in Sections 5 and 6, respectively. Finally conclusions are given in Section 7.

2. BASE DISTURBANCE MODEL

The disturbance observer is famous for its simplicity and relatively powerful performance for compensating the disturbance in lumped form and even the parametric error. For that reason, it has been applied to various area [21–25]. General structure of the disturbance observer is depicted in Fig. 1. As mentioned in the introduction and described in Fig. 2, however, the disturbance observer has a limitation in compensating for the lumped disturbance at high speed operating conditions, because of both the position dependent property of the force ripple and the upper limit of the Q-filter bandwidth. As an alternative, we suggested a feed-forward disturbance compensation method in [2]. The method can be summarized as follows. First, some experiments are conducted at constant but various speed conditions with the disturbance observer. Then, the output signal of the disturbance observer is analyzed offline through the auto-correlation, fast Fourier transform and averaging. Finally, the coefficients of the sinusoidal lumped disturbance are acquired as a function of position.

In the above described method, disturbance information for the feed-forward compensation is given as a function of position. This creates a consistent performance in disturbance compensation regardless of the traveling speed, differently from the disturbance observer.

In fact, some delay is included in the previous position dependent disturbance model because it is acquired by off-

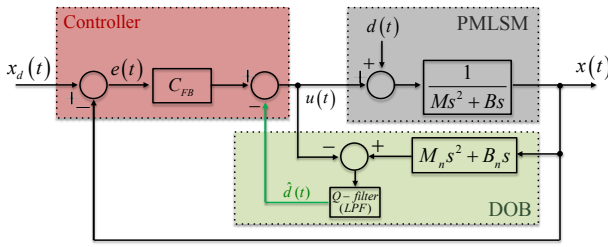


Fig. 1. General structure of disturbance observer.

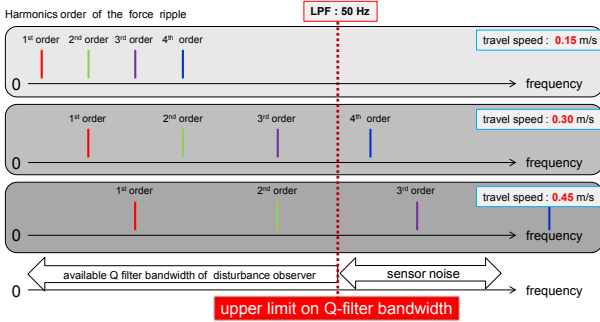


Fig. 2. Limitation of disturbance observer at high traveling speed.

line analysis with the disturbance observer output, which is passed through a Q-filter. However this can be compensated by initial position estimation using an extended Kalman filter, which will be discussed in the following section.

For the continuity of sinusoidal position dependent disturbance model at each boundary of the permanent magnets, some smoothing of the disturbance model was applied within the ± 1 mm region of each boundary.

3. EXTENDED KALMAN FILTER DESIGN

Due to nonlinear property of the lumped disturbance model (i.e., the sinusoidal characteristic), an extended Kalman filter is adopted for adaptive control. In our previous research [2], we concluded that the disturbance in the permanent magnet linear motor system is supposed to be eliminated more than 75% by accurate compensation of up to the 2nd order harmonics, more than 87% by up to the 4th order harmonics and more than 93% by up to the 6th order harmonics. Considering the effect and computation time, 0 to 4th order harmonics are modeled for the feed-forward compensation.

Fig. 3 shows the coefficients of DC, 1st order harmonics cosine, 2nd order harmonics cosine and 3rd order harmonics cosine along the magnet position (i.e., along the moving direction of the motor). The coefficients of the sine component and the 4th order harmonics are omitted in the figure. The colored dotted lines show the experimental

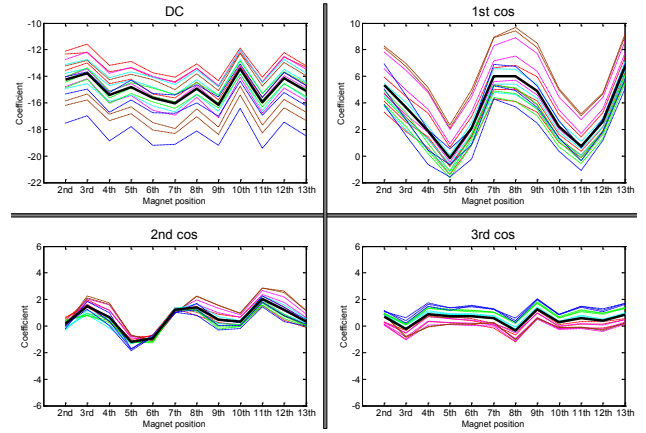


Fig. 3. Experimental analysis and average of coefficient along the magnet position. (colored dotted line : experimental data, bold black line : average).

18 data sets and the bold black line presents the average, which is identical to the position dependent lumped disturbance model described in the previous section. As can be seen easily in the figure, the variation from the average is relatively small in the case of the 2nd, 3rd and 4th (though the 4th is omitted in the figure) compared with that of the DC and 1st. Thus, to reduce the computational burden, the real time offset error from the lumped disturbance model of only the DC and 1st order harmonics term will be adapted by extended Kalman filter. In other words, the 2nd, 3rd and 4th order harmonics components are not adapted. And the coefficient adaptation scheme is enacted by adding the difference between the feed-forward model and the real value rather than by multiplying the ratio between them. This is because some coefficient values are close to zero and the overall shape seems to overlap very well by adding some offset.

The dynamics of the motor mechanical system is given by

$$M\ddot{x}(t) + B\dot{x}(t) = u(t) + d(t), \quad (1)$$

where M is the mass of the mover, B the viscous friction coefficient, $x(t)$ the position of the mover, $u(t)$ the thrust force and $d(t)$ the lumped disturbance including the detent force and the friction force as well as external disturbance. Assuming that the lumped disturbance consists of up to the 4th order harmonics, $d(t)$ in (1) can be decomposed as follows:

$$\begin{aligned} d(t) = & \left[(C_{A0} + C_0) + (C_{A1} + C_1) \cdot \cos\left(\frac{2\pi}{x_{pp}}(x + x_s)\right) \right. \\ & + (C_{A2} + C_2) \cdot \sin\left(\frac{2\pi}{x_{pp}}(x + x_s)\right) \\ & \left. + C_3 \cdot \cos\left(\frac{2\pi}{x_{pp}}(x + x_s) * 2\right) + C_4 \cdot \sin\left(\frac{2\pi}{x_{pp}}(x + x_s) * 2\right) \right] \end{aligned}$$

$$\begin{aligned}
& + C_5 \cdot \cos\left(\frac{2\pi}{x_{pp}}(x+x_s) * 3\right) + C_6 \cdot \sin\left(\frac{2\pi}{x_{pp}}(x+x_s) * 3\right) \\
& + C_7 \cdot \cos\left(\frac{2\pi}{x_{pp}}(x+x_s) * 4\right) + C_8 \cdot \sin\left(\frac{2\pi}{x_{pp}}(x+x_s) * 4\right) \Big], \quad (2)
\end{aligned}$$

where C_{A0} , C_{A1} and C_{A2} are the coefficient errors to be adapted by the extended Kalman filter, $C_0 \sim C_8$ the coefficients of the position dependent disturbance model for feed-forward compensation, x_{pp} is the pole pitch of the permanent magnets and x_s the initial position that is to be estimated by the extended Kalman filter.

The variable x for the extended Kalman filter is chosen as follows:

$$x = \begin{bmatrix} x_1 \\ x_2 \\ x_3 \\ x_4 \\ x_5 \\ x_6 \end{bmatrix} = \begin{bmatrix} x \\ \dot{x} \\ x+x_s \\ C_{A0} \\ C_{A1} \\ C_{A2} \end{bmatrix}, \quad (3)$$

then the state space representation is given by

$$\begin{aligned}
\dot{x}_1 &= x_2, \\
\dot{x}_2 &= -\frac{B}{M}x_2 + \frac{1}{M}u + \left[\frac{(x_4 + C_0)}{M} \right. \\
& + \frac{(x_5 + C_1)}{M} \cos\left(\frac{2\pi}{x_{pp}}(x_3)\right) + \frac{(x_6 + C_2)}{M} \sin\left(\frac{2\pi}{x_{pp}}(x_3)\right) \\
& + \frac{C_3}{M} \cos\left(\frac{2\pi}{x_{pp}}(x_3) * 2\right) + \frac{C_4}{M} \sin\left(\frac{2\pi}{x_{pp}}(x_3) * 2\right) \\
& + \frac{C_5}{M} \cos\left(\frac{2\pi}{x_{pp}}(x_3) * 3\right) + \frac{C_6}{M} \sin\left(\frac{2\pi}{x_{pp}}(x_3) * 3\right) \\
& \left. + \frac{C_7}{M} \cos\left(\frac{2\pi}{x_{pp}}(x_3) * 4\right) + \frac{C_8}{M} \sin\left(\frac{2\pi}{x_{pp}}(x_3) * 4\right) \right], \\
\dot{x}_3 &= x_2, \\
\dot{x}_4 &= 0, \\
\dot{x}_5 &= 0, \\
\dot{x}_6 &= 0, \quad (4)
\end{aligned}$$

where it is assumed that $\dot{x}_s \simeq 0$, $\dot{C}_{A0} \simeq 0$, $\dot{C}_{A1} \simeq 0$ and $\dot{C}_{A2} \simeq 0$. This seems reasonable from Fig. 3. In that figure, the offset value itself is different by cases, but the variation along the magnet position is small.

Using forward rectangular approximation, (4) is discretized as follows:

$$\begin{aligned}
x_1(k+1) &= x_1(k) + T_s x_2(k), \\
x_2(k+1) &= \left(1 - \frac{T_s B}{M}\right) x_2(k) + \frac{T_s}{M} u(k+1) \\
& + \frac{T_s(x_4(k) + C_0)}{M} + \frac{T_s(x_5(k) + C_1)}{M} \cos\left(\frac{2\pi}{x_{pp}} x_3(k)\right) \\
& + \frac{T_s(x_6(k) + C_2)}{M} \sin\left(\frac{2\pi}{x_{pp}} x_3(k)\right)
\end{aligned}$$

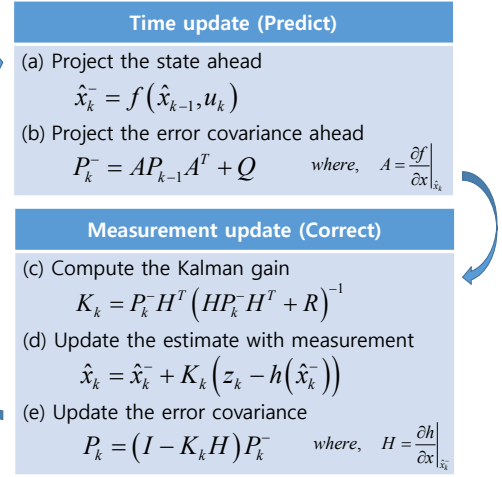


Fig. 4. Process of the extended Kalman filter.

$$\begin{aligned}
& + \frac{T_s C_3}{M} \cos\left(\frac{2\pi}{x_{pp}} x_3(k) * 2\right) + \frac{T_s C_4}{M} \sin\left(\frac{2\pi}{x_{pp}} x_3(k) * 2\right) \\
& + \frac{T_s C_5}{M} \cos\left(\frac{2\pi}{x_{pp}} x_3(k) * 3\right) + \frac{T_s C_6}{M} \sin\left(\frac{2\pi}{x_{pp}} x_3(k) * 3\right) \\
& + \frac{T_s C_7}{M} \cos\left(\frac{2\pi}{x_{pp}} x_3(k) * 4\right) + \frac{T_s C_8}{M} \sin\left(\frac{2\pi}{x_{pp}} x_3(k) * 4\right), \\
x_3(k+1) &= x_3(k) + T_s x_2(k), \\
x_4(k+1) &= x_4(k), \\
x_5(k+1) &= x_5(k), \\
x_6(k+1) &= x_6(k), \quad (5)
\end{aligned}$$

where T_s is the sampling time. The design parameters for the extended Kalman filter are chosen as follows:

$$\begin{aligned}
\hat{x}_0 &= [0 \ 0 \ 0 \ 0 \ 0 \ 0]^T, \\
\text{diag}(P_0) &= [10^{-4} \ 10^{-4} \ 10^5 \ 10^8 \ 10^6 \ 10^3], \\
\text{diag}(Q) &= [10^{-4} \ 10^3 \ 10^{-1} \ 10^6 \ 10^8 \ 10^7], \\
R &= [10^{-2}], \\
H &= [1 \ 0 \ 0 \ 0 \ 0 \ 0], \quad (6)
\end{aligned}$$

where \hat{x}_0 is an estimate of the initial state, P_0 the error covariance matrix of the initial state, Q the system noise covariance matrix, R the measurement noise covariance matrix and H the output matrix.

In general, the extended Kalman filter consists of mainly two procedures, the 'Time update (Predict)' and the 'Measurement update (Correct)' as shown in Fig. 4. With the tuning parameters in (6), the variable x is recursively calculated through those processes.

The entire structure including the proposed extended Kalman filter is shown in Fig. 5. In the figure, C_{PID_FB} means a proportional integral derivative (PID) feedback controller, C_{IPM_FF} a inverted plant model (IPM) feed-forward controller and C_{dist_FF} a feed-forward disturbance compensator.

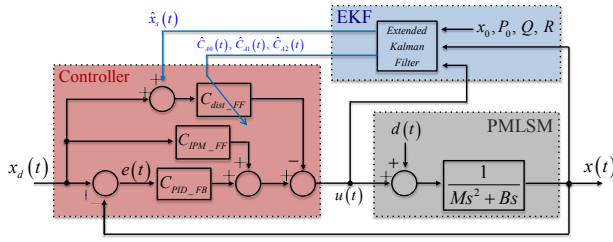


Fig. 5. Entire structure with EKF for initial position estimation and coefficients adaptation.

In fact, in a real system (i.e., in a practical environment), the viscous friction coefficient B in (5) changes with time due to dust, rust, subtle deformation and so on. The mover mass M can also be changed depending on the load. However, in those cases, with this suggested method, there is no need to redo the disturbance identification work. In other words, it is neither necessary to reconstruct the feed-forward model itself nor redesign the extended Kalman filter. Just redefining M and B with new ones is enough. This is a very convenient and advantageous point compared with the curve fitting method [13] or the look up table scheme [4, 15].

4. RECURSIVE LEAST SQUARES ALGORITHM AND DELTA DISTURBANCE OBSERVER DESIGN

As a comparative method to the suggested extended Kalman filter, the recursive least squares filter [6] and a modified version of the disturbance observer [10–12, 16] have been constructed.

4.1. Recursive least squares filter design

The general structure of the recursive least squares filter as in [6] is given by

$$d = \begin{bmatrix} 1 & \cos\left(\frac{2\pi}{x_{pp}}x\right) & \sin\left(\frac{2\pi}{x_{pp}}x\right) \end{bmatrix} \begin{bmatrix} C_{DC} \\ C_{1\cos} \\ C_{1\sin} \end{bmatrix} + v, \quad (7)$$

where C_{DC} is the coefficient of the DC term, $C_{1\cos}$ the cosine coefficient of the 1st order harmonics, $C_{1\sin}$ the sine coefficient of the 1st order harmonics and v the measurement noise. However, with (7), at the boundary of each permanent magnet, where the coefficients vary immediately, the adaptation response is slow and the tracking error becomes larger. To solve this problem and also fully utilize the information available, a modified version is de-

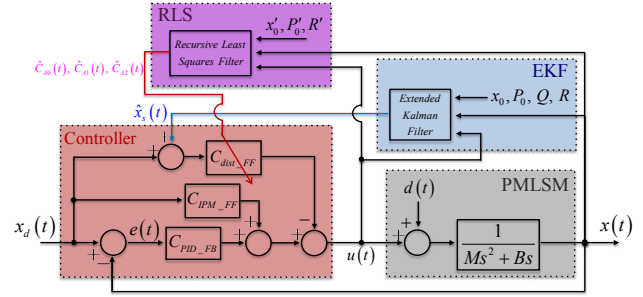


Fig. 6. Entire structure with EKF for initial position estimation and RLS for coefficients adaptation.

vised as follows:

$$d = \begin{bmatrix} C_0 & C_1 \cos\left(\frac{2\pi}{x_{pp}}x\right) & C_2 \sin\left(\frac{2\pi}{x_{pp}}x\right) \end{bmatrix} \begin{bmatrix} G_{A0} \\ G_{A1} \\ G_{A2} \end{bmatrix} + v, \quad (8)$$

where C_0 , C_1 and C_2 are the feed-forward disturbance model coefficients identical to those in (2), and G_{A0} , G_{A1} and G_{A2} the factors to be multiplied to the feed-forward model, respectively. The design parameter for the recursive least squares filter in (8) is chosen as follows:

$$\hat{x}_0 = \begin{bmatrix} 1 \\ 1 \\ 1 \end{bmatrix}, \quad P_0 = \begin{bmatrix} 3 & 0 & 0 \\ 0 & 3 & 0 \\ 0 & 0 & 1 \end{bmatrix}, \quad R = [10^{+0}], \quad (9)$$

where \hat{x}_0 is the initial estimate of G_{A0} , G_{A1} and G_{A2} .

This recursive least squares filter is for the adaptation of disturbance model coefficients in (2) and not for the initial position estimation. Therefore, for an impartial comparison with the suggested extended Kalman filter, the starting point estimation algorithm in the extended Kalman filter is adopted. The entire block diagram of this control scheme is depicted in Fig. 6.

4.2. Delta disturbance observer design

The typical structure of the disturbance observer was already shown in Fig. 1. The general role of the disturbance observer is to compensate for the entire disturbance at once as in that figure. However, there are some shortcomings with the disturbance observer: magnitude reduction near the cutoff frequency of the Q-filter and a phase lag.

To overcome these limitations and for the full application of available disturbance information, a delta disturbance observer is designed. As can be seen in Fig. 7, the *delta*(Δ) means the difference between the feed-forward disturbance model C_{dist_FF} and the real disturbance d . By adopting this delta disturbance observer with an identical Q-filter bandwidth, the reduction amount among the disturbance to be compensated can be decreased compared

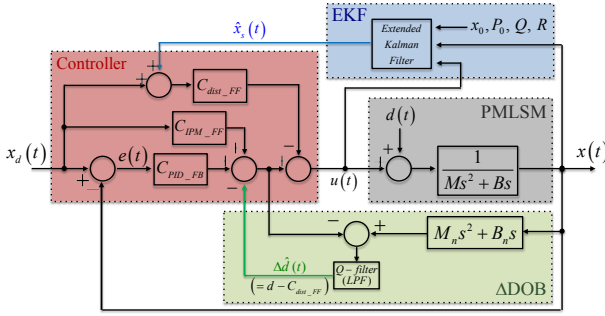


Fig. 7. Entire structure with EKF for initial position estimation and Δ DOB.

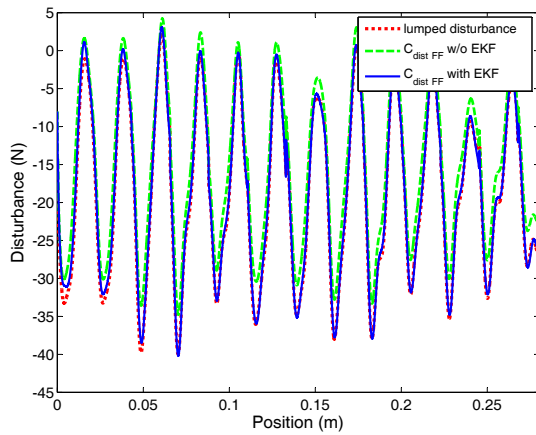


Fig. 8. Simulation result of lumped disturbance shape.

to that of general disturbance observer described in Fig. 1. In other words, even though the reduction ratio is fixed by the same cutoff frequency of the Q-filter, the reduction amount can be cut down along with the less amount of input entering the Q-filter.

5. SIMULATION RESULTS

Prior to experimental validation, we conducted simulations. The extended Kalman filter is designed as described in section III. The disturbance observer output of one experiment data is employed as the virtual lumped disturbance d .

The simulation results are shown in Fig. 8 and Fig. 9. In those figures, the red dotted line, green dashed line and blue solid line indicate the virtual disturbance, feed-forward compensation without the extended Kalman filter and with the extended Kalman filter, respectively. Fig. 8 shows how the suggested extended Kalman filter identifies the lumped disturbance effectively. As explained in Section 3, one of the two roles of the proposed extended Kalman filter is to provide accurate coefficients of the DC and 1st order harmonics. Fig. 9 shows that the disturbance coefficient adaptation scheme is working very fast.

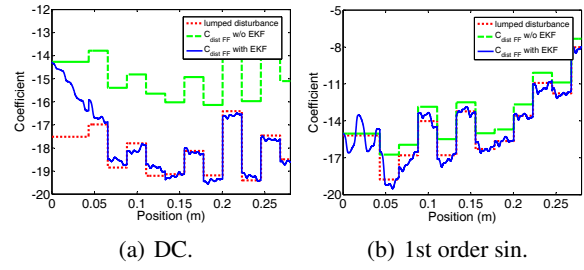


Fig. 9. Simulation result of lumped disturbance coefficient: (a) DC component. (b) 1st order sin harmonics.

6. EXPERIMENTAL RESULTS

To verify the control schemes described in the previous sections, we performed experiments using a permanent magnet linear synchronous motor system.

6.1. Experimental setup

All the experiments were carried out with the prototype permanent magnet linear synchronous motor system depicted in Fig. 10. The system parameters are given in Table 1. These parameters were obtained by a system identification method which is not described in this paper. The PWM inverter used for the experiments had 10kHz switching frequency and was controlled by a dSPACE DS 1103 board. The current and position controls were executed at 50 μ sec and 0.5msec loop time, respectively. An optical linear encoder, which had a resolution of 0.5 μ m, was installed to measure the position of the mover.

As mentioned in Section 2, the proposed feed-forward disturbance compensation scheme has an advantage, especially at a faster traveling speed, where the position dependent force ripple frequency is increased proportional to the speed, while the disturbance observer shows poor performance due to the limitation of the Q-filter bandwidth.



Fig. 10. Experimental prototype PMLSM system.

Table 1. Parameters of the PMLSM system.

Parameter	Symbol	Value	Unit
Mover mass	M	6.70	kg
Viscous friction coefficient	B	57.7	N/m/s
Pole pitch	x_p	22.5	mm

The maximum Q-filter bandwidth available with the motor system depicted in Fig. 10 is about 50Hz . We chose the 1.4 times of the first order harmonic as the Q-filter bandwidth for the delta disturbance observer considering that the proposed extended Kalman filter adapts up to the 1st order harmonics. With a pole pitch of 22.5 mm , the mover speed equivalent to the 1.4 times of the first order harmonic at 50 Hz is calculated as 0.80 m/s . This operating speed of 0.80 m/s is practical for many industrial applications.

Considering the maximum travel distance of the mover in the experimental prototype which is only 0.5 m , the travel distance of the mover is limited to about 0.4 m . Meanwhile, it is assumed that the position dependent force ripple composes most of the lumped disturbance, the Coulomb friction is constant and its speed dependent variation can be adapted by the DC component of the extended Kalman filter. From those limitation and assumption, the experiments are performed with the speed scaled down by the factor of 10, i.e., the travel speed of 0.08 m/s and the Q-filter bandwidth of 5 Hz .

6.2. Verification of suggested method

A list of all the experiments and the applied control schemes are summarized in Table 2, where ' Q_{\square} ' in DOB denotes the corresponding harmonics order of the Q-filter bandwidth, '*gen*' and '*sug*' in RLS indicate the general RLS (7) and the suggested RLS (8) respectively, and ' ΔDOB ' is the delta disturbance observer shown in Fig. 7. In the case of '*1st only*' in EKF, $C_0 \sim C_8$ described in Section 3 are the constants fitted using the first magnet (i.e., given as position-invariant constants), thus the coefficient errors for other magnets are larger and should be compensated by $C_{A0} \sim C_{A2}$ of EKF, while those of '*full*' version are given as a function of position (i.e., the position dependent constants) as shown in Fig. 3. In other words, '*1st only*' version can reduce the memory for EKF, but the error is increased, whereas '*full*' version has better performance by utilizing all the information available.

As already shown in Fig. 6 and Fig. 7, the proportional integral derivative (PID) feedback controller $C_{\text{PID_FB}}$ and the inverted plant model (IPM) feed-forward controller $C_{\text{IPM_FF}}$ are commonly applied to all the eight cases.

From the disturbance compensation point of view, the first three cases in Table 2 utilize the general disturbance observer as shown in Fig. 1. The remaining five cases basically adopt the position dependent feed-forward disturbance model (dist FF), and the disturbance error is compensated by different ways (e.g., RLS, ΔDOB , EKF). Meanwhile, since the position data is acquired from an incremental encoder, the information of the initial starting position is necessary. Therefore, for an equitable evaluation of the coefficients adaptation schemes, the initial position correction algorithm of EKF is applied to all the five cases.

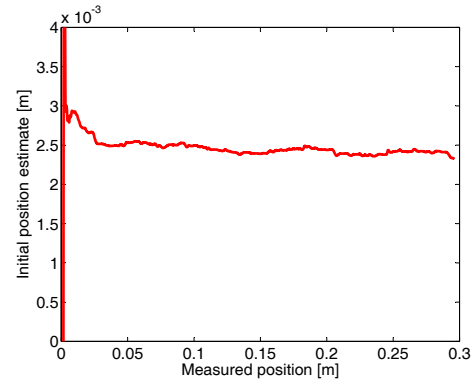


Fig. 11. Initial starting position estimate.

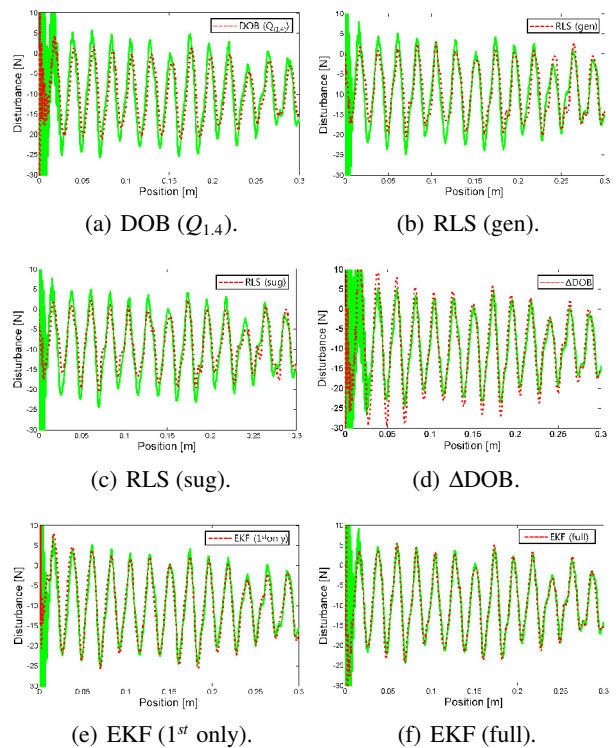


Fig. 12. Lumped disturbance comparison.

Fig. 11 shows the initial starting position estimated by EKF. As mentioned above, to exclude the effect of the initial position error on the coefficient adaptation ability, data after convergence (e.g., after 0.15 m in the figure) are used for following performance analysis.

Fig. 12 compares the performance of different disturbance estimation schemes. In the figure, the green solid line represents the real lumped disturbance. Since the true lumped disturbance is unknown, the disturbance observer output through the Q-filter with bandwidth equivalent to the 10th order harmonics is assumed as the real disturbance. (This is another reason to experiment at the traveling speed of 0.08 m/s rather than 0.8 m/s). As can be seen easily in the figure, the solo disturbance ob-

Table 2. Experiments list and applied control schemes.

Controller Types	Disturbance model		Initial position correction	Coefficient adaptation	Remarks
	1 st magnet only	Full magnets			
DOB ($Q_{1.4}$)					Q filter bandwidth : $1.4*FH^1$
DOB (Q_2)					Q filter bandwidth : $2*FH^1$
DOB (Q_3)					Q filter bandwidth : $3*FH^1$
RLS (gen)		✓	✓	✓	General RLS (7)
RLS (sug)		✓	✓	✓	Suggested RLS (8)
Δ DOB		✓	✓		Delta disturbance observer
EKF (1 st only)	✓		✓	✓	position-invariant coefficients
EKF (full)		✓	✓	✓	position dependent coefficients

¹⁾ FH : Fundamental harmonic

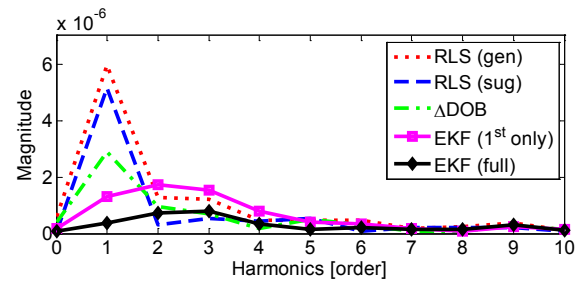
Table 3. RMS error comparison.

	RMS error
DOB ($Q_{1.4}$)	8.6451 μm
DOB (Q_2)	7.4039 μm
DOB (Q_3)	5.3202 μm
RLS (gen)	4.8756 μm
RLS (sug)	4.0657 μm
Δ DOB	2.6715 μm
EKF (1 st only)	2.9972 μm
EKF (full)	1.3545 μm

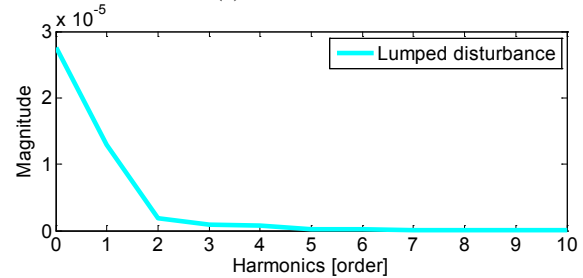
server (Fig. 12(a)) has the worst performance even with some phase lag, and the suggested 'full' version extended Kalman filter (Fig. 12(f)) demonstrates the best performance as expected.

The RMS error of each control scheme is given in Table 3. Similarly to the result in Fig. 12, the proposed 'full' version extended Kalman filter shows the least amount of RMS error. The recursive least squares method does not perform well as the extended Kalman filter for the following reasons. The difference in coefficients between the real disturbance and the disturbance model (dist FF) can be expressed as the offset as shown in Fig. 3. However, in the recursive least squares method as given by (7) or (8), the coefficient errors are compensated by the ratio between the real value and the model, and that ratio will be changed drastically if the real value is quite small. As can be seen in Fig. 3, there are indeed some values near zero. On the other hand, from the result of Fig. 12 and Table 3, the extended Kalman filter of the '1st only' version shows better performance than the recursive least squares method. However, the RMS error is more than twice larger than that of 'full' version. As the variation between consecutive ripples becomes greater, the RMS error of the '1st only' version also gets larger. This confirms that the 'full' version of the extended Kalman filter is necessary for more precise motion control.

Finally, we conducted a fast Fourier transform analysis on the position error, and for an additional comparison,



(a) Position error.



(b) Lumped disturbance.

Fig. 13. FFT analysis on: (a) position error and (b) lumped disturbance.

we also analyzed the uncompensated raw lumped disturbance. The results are shown in Fig. 13. It is necessary to pay attention to the scale: (b) is 10 times larger than (a). As can be seen easily in the figure, all the compensating schemes are good at DC component rejection. However, the recursive least squares method shows relatively poor performance for the 1st order harmonics. As mentioned earlier, this is because of the near-zero values of the disturbance coefficient. In addition, the '1st only' version extended Kalman filter has the maximum error among the five control schemes at the 2nd, 3rd and 4th order harmonics. This result is as expected since the coefficient errors of the 2nd ~ 4th order harmonics are not adapted in the '1st only' version and also the coefficients are not varying position dependently, whereas the other four control schemes are working with position dependent varying coefficients.

7. CONCLUSION

Continuing our previous research on finding the lumped disturbance model as a position dependent function using the simple disturbance observer at a relatively low traveling speed where higher harmonics can be detected with a fixed Q-filter bandwidth, we designed an adaptive controller using an extended Kalman filter for a feed-forward disturbance compensator as follows. First, the initial starting position of the translator is estimated and reflected to the feed-forward model. This is important for the feed-forward position controller since general linear motor systems are usually equipped with an incremental encoder for the sake of ultra high resolution. Second, the coefficients of the disturbance model up to the 1st order harmonics are adjusted by the extended Kalman filter and compared with other control schemes such as the disturbance observer and the recursive least squares method. It is verified that the proposed extended Kalman filter has superior performance in disturbance compensation and adaptation in terms of the RMS position error and FFT analysis on the position error signal.

Also using the suggested method, the Coulomb friction force is compensated since the DC component is included in the disturbance model and is adapted by the extended Kalman filter. Accordingly, by combining the developed compensation method with an appropriate static friction and Stribeck effect model, even higher precision motion control for arbitrary reference trajectory is expected to be achievable.

REFERENCES

- [1] B. Armstrong, P. Dupont, and C. C. D. WIT, "A survey of models, analysis tools and compensation methods for the control of machines with friction," *Automatica*, vol. 30, pp. 1083-1138, 1994. [click]
- [2] J. Kim, K. Cho, H. Jung, and S. Choi, "A novel method on disturbance analysis and feed-forward compensation in permanent magnet linear motor system," *Proc. IEEE Fifth Int. Conf. Intell. Syst. Modeling Simulation*, pp. 394-399, 2014.
- [3] H. Jang, *The Compensation of Torque Ripple of Brushless DC Motor using Feedforward Method*, Master thesis, KAIST, Korean, 2006.
- [4] L. Bascetta, P. Rocco, and G. Magnani, "Force ripple compensation in linear motors based on closed-loop position-dependent identification," *IEEE/ASME Trans. Mechatronics*, vol. 15, no. 3, pp. 349-359, 2010. [click]
- [5] S. Chen, K. K. Tan, S. Huang, and C. S. Teo, "Modeling and compensation of ripples and friction in permanent-magnet linear motor using a hysteretic relay," *IEEE/ASME Trans. Mechatronics*, vol. 15, no. 4, pp. 586-594, 2010. [click]
- [6] S. Zhao and K. K. Tan, "Adaptive feedforward compensation of force ripples in linear motors," *Control Eng. Practice* vol. 13, no. 9, pp. 1081-1092, 2005. [click]
- [7] K. K. Tan, T. H. Lee, H. Dou, and S. Zhao, "Force ripple suppression in iron-core permanent magnet linear motors using an adaptive dither," *J. Franklin Inst.*, vol. 341, no. 4, pp. 375-390, 2004. [click]
- [8] K. K. Tan, S. N. Huang, and T. H. Lee, "Robust adaptive numerical compensation for friction and force ripple in permanent-magnet linear motors," *IEEE Trans. Magn.*, vol. 38, no. 1, pp. 221-228, 2002. [click]
- [9] Y. Zhu, S. Jin, K. Chung, and Y. Cho, "Control-based reduction of detent force for permanent magnet linear synchronous motor," *IEEE Trans. Magn.*, vol. 45, no. 6, pp. 2827-2830, 2009. [click]
- [10] W. Su and C. Liaw, "Adaptive positioning control for a LPMSM drive based on adapted inverse model and robust disturbance observer," *IEEE Trans. Power Electron.*, vol. 21, no. 2, pp. 505-517, 2006. [click]
- [11] M. Yan and Y. Shiu, "Theory and application of a combined feedback-feedforward control and disturbance observer in linear motor drive wire-EDM machines," *Int. J. Mach. Tools Manuf.*, vol. 48, pp. 388-401, 2008. [click]
- [12] M. Yan, K. Huang, Y. Shiu, and Y. Chen, "Disturbance observer and adaptive controller design for a linear-motor-driven table system," *Int. J. Adv. Manuf. Technol.*, vol. 35, pp. 408-415, 2007. [click]
- [13] C. Rohrig and A. Jochheim, "Identification and compensation of force ripple in linear permanent magnet motors," *Proc. Amer. Control Conf.*, pp. 2161-2166, 2001.
- [14] H. Stearns, S. Mishra, and M. Tomizuka, "Iterative tuning of feedforward controller with force ripple compensation for wafer stage," *Proc. IEEE Int. Workshop Adv. Motion Control*, pp. 234-239, 2008. [click]
- [15] Y. Zhu, D. Koo, and Y. Cho, "Detent force minimization of permanent magnet linear synchronous motor by means of two different methods," *IEEE Trans. Magn.*, vol. 44, no. 11, pp. 4345-4348, 2008. [click]
- [16] K. K. Tan, T. H. Lee, H. F. Dou, S. J. Chin, and S. Zhao, "Precision motion control with disturbance observer for pulsewidth-modulated-driven permanent-magnet linear motors," *IEEE Trans. Magn.*, vol. 39, no. 3, pp. 1813-1818, 2003. [click]
- [17] E. A. Wan and R. v. d. Merwe, "The unscented Kalman filter for nonlinear estimation," *Proc. IEEE Symp. Adaptive Syst. Signal Process., Commun. Control.*, pp. 153-158, 2000.
- [18] M. S. Arulampalam, S. Maskell, N. Gordon, and T. Clapp, "A tutorial on particle filters for online nonlinear/non-Gaussian Bayesian tracking," *IEEE Trans. Signal Process.*, vol. 50, no. 2, pp. 174-188, 2002. [click]
- [19] B. Liu and I. Hoteit, "Nonlinear Bayesian mode filtering," *Int. J. Innovative Comput., Inf. Control*, vol. 11, no. 1, pp. 231-245, 2015.
- [20] F. Daum, "Nonlinear filters: beyond the Kalman filter," *IEEE Trans. Aerosp. Electron. Syst. Mag.*, vol. 20, no. 8, pp. 57-69, 2005.

- [21] M. A. Janaideh and A. H. EL-Shaer, "Performance enhancement for a class of hysteresis nonlinearities using disturbance observers," *International Journal of Control, Automation, and Systems*, vol. 12, no. 2, pp. 283-293, 2014. [click]
- [22] M. Chen and B. Jiang, "Robust attitude control of near space vehicles with time-varying disturbances," *International Journal of Control, Automation, and Systems*, vol. 11, no. 1, pp. 182-187, 2013. [click]
- [23] J. Seok, W. Yoo, and S. Won, "Inertia-related coupling torque compensator for disturbance observer based position control of robotic manipulators," *International Journal of Control, Automation, and Systems*, vol. 10, no. 4, pp. 753-760, 2012. [click]
- [24] X. Chen, J. Li, J. Yang, and S. Li, "A disturbance observer enhanced composite cascade control with experimental studies," *International Journal of Control, Automation, and Systems*, vol. 11, no. 3, pp. 555-562, 2013. [click]
- [25] K. Kong and M. Tomizuka, "Nominal model manipulation for enhancement of stability robustness for disturbance observer-based control systems," *International Journal of Control, Automation, and Systems*, vol. 11, no. 1, pp. 12-20, 2013. [click]



Jonghwa Kim received his B.S. degree in materials engineering from Hokkaido University, Sapporo, Japan, the M.S. degree in mechanical engineering from the Korea Advanced Institute of Science and Technology (KAIST), Daejeon, Korea, in 2009. His research interests include control theory and its application.



Kwanghyun Cho received his B.S. degree in electrical engineering from Kyungpook National University, Daegu, Korea, his M.S. and Ph.D. degrees in mechanical engineering from the Korea Advanced Institute of Science and Technology (KAIST), Daejeon, Korea, in 2014. His research interests include high precision motion control.



Seibum Choi received his B.S. degree in mechanical engineering from Seoul National University, Seoul, Korea, an M.S. degree in mechanical engineering from the Korea Advanced Institute of Science and Technology (KAIST), Daejeon, Korea, and a Ph.D. degree in control from the University of California, Berkeley, CA, USA, in 1993. His research interests include vehicle dynamics and control and fuel-saving technology.